submitted to ApJ

# Recent X-ray Variability of $\eta$ Carinae: the Quick Road to Recovery

M. F. Corcoran[1,2], K. Hamaguchi[1,3], J. M. Pittard[4], C. M. P. Russell[5], S. P. Owocki[5], E. R. Parkin[6], A. Okazaki[7]

## ABSTRACT

We report continued monitoring of the superluminous binary system $\eta$ Car by the Proportional Counter Array on the Rossi X-ray Timing Observatory (*RXTE*) through the 2009 X-ray minimum. The *RXTE* campaign shows that the minimum began on 2009 January 16, consistent with the phasings of the two previous minima, and overall, the temporal behavior of the X-ray emission was similar to that observed by *RXTE* in the previous two cycles. However, important differences did occur. The 2–10 keV X-ray flux and X-ray hardness decreased in the 2.5-year interval leading up to the 2009 minimum compared to the previous cycle. Most intriguingly, the 2009 X-ray minimum was about one month shorter than either of the previous two minima. During the egress from the 2009 minimum the X-ray hardness increased markedly as it had during egress from the previous two minima, although the maximum X-ray hardness achieved was less than the maximum observed after the two previous recoveries. We suggest that the cycle-to-cycle variations, especially the unexpectedly early recovery from the

[1]CRESST and X-ray Astrophysics Laboratory, NASA/Goddard Space Flight Center, Greenbelt, MD 20771

[2]Universities Space Research Association, 10211 Wincopin Circle, Suite 500 Columbia, MD 21044, USA.

[3]Department of Physics, University of Maryland, Baltimore County, 1000 Hilltop Circle, Baltimore, MD 21250, USA

[4]School of Physics and Astronomy, The University of Leeds, Leeds LS2 9JT

[5]Bartol Research Institute, Department of Physics & Astronomy, University of Delaware, Newark, DE 19716, USA

[6]Institut d'Astrophysique et de Géophysique, Université de Liège, 17, Allée du 6 Août, B5c, B-4000 Sart Tilman, Belgium

[7]Faculty of Engineering, Hokkai-Gakuen University, Toyohira-ku, Sapporo 062-8605, Japan

2009 X-ray minimum, might have been the result of a decline in $\eta$ Car's wind momentum flux produced by a drop in $\eta$ Car's mass loss rate or wind terminal velocity (or some combination), though if so the change in wind momentum flux required to match the X-ray variation is surprisingly large.

*Subject headings:* X-rays: stars – stars: early-type – stars: individual ($\eta$ Car) – stars: LBV

## 1. Introduction

$\eta$ Car is the closest example of a superluminous, supermassive star near $100 M_{\odot}$ (Davidson & Humphreys 1997; Hillier et al. 2001). The star is near the Eddington limit, and as such it is unstable, and prone to sporadic episodes of large mass loss such as the "Great Eruption" in the mid-$19^{th}$ century which generated massive ejecta at speeds of up to 6000 km s$^{-1}$, producing almost as much kinetic energy as a low-luminosity supernova (Smith 2008). Key questions are whether $\eta$ Car and those rare stars like it are close to exploding (Smith et al. 2007), how they will explode, and what they will leave behind. The answer to these questions depends on stellar mass and angular momentum, and changes in these quantities. As noted by Langer (1998), for massive stars, stellar mass loss, angular momentum loss and stellar evolution are tightly coupled. For single massive stars, mass loss via radiatively-driven stellar winds will remove angular momentum. In binary star systems, the presence of a companion can affect wind-driven mass loss and also can provide alternative pathways for the exchange of mass and angular momentum.

Observations over the past few decades (see Damineli et al. 2008, and references therein) provide strong, if not conclusive, evidence that $\eta$ Car is orbited by a companion star. The existence of a companion star in orbit around $\eta$ Car can in principle play a significant role in the evolution of mass and angular momentum of the system. The companion also acts as an in-situ probe of the massive wind from $\eta$ Car, while at the same time perturbing that wind. The presence of a hot companion star is inferred indirectly from well-defined changes in the excitation of the circumstellar gas produced when the UV radiation from the companion becomes absorbed by the thick inner wind of $\eta$ Car near the time of periastron passage. In this scenario, X-rays are the natural consequence of the collision of the companion's fast stellar wind ($V_{\infty} \approx 3000$ km s$^{-1}$, Pittard & Corcoran 2002) against the slower, denser wind of $\eta$ Car ($V_{\infty} \approx 500$ km s$^{-1}$, Hillier et al. 2001), resulting in a strong shock with a post-shock temperature peak near 50 million K. Variable X-ray emission (Ishibashi et al. 1999; Corcoran 2005) will be dominated by orbital phase-dependent changes in the emission measure of the hot shocked companion wind along with changes in intervening X-ray absorption provided

by the wind of $\eta$ Car, as the companion moves around $\eta$ Car in one of the most eccentric orbits in stellar astrophysics (see for example Parkin et al. 2009, and references therein). The X-rays fade to a short minimum state which may be produced by the occultation or eclipse of the shocked companion wind by the wind (and photosphere?) of $\eta$ Car, and/or the intrinsic disruption of the colliding wind shock near periastron. Since the companion star is not directly detected, the cyclical X-ray variations play an important role in determining the orbital and stellar parameters of the system.

Here we present *RXTE* (Bradt et al. 1993) X-ray observations through July 2009 that show significant changes compared to the previous two cycles, and most surprisingly reveal that the X-ray flux in the 2–10 keV band increased about 1 month prior to expected recovery. In Section 2, we describe the *RXTE* X-ray observations. Section 3 compares the X-ray brightness from the three cycles so far observed by *RXTE*, while section 4 compares the cyclical changes in X-ray hardness. In section 5 we discuss variations of spatially-resolved X-ray spectra at two key phases separated by one complete cycle as a detailed characterization of the cycle-to-cycle X-ray variations, while a discussion of the observations and our interpetations are given in Section 6. Finally we summarize our conclusions in Section 7.

## 2. The *RXTE* Observations

The *RXTE* observations reported here are through 2009 July 30 inclusive[1]. The data were obtained by the *RXTE* Proportional Counter Array (PCA), and we consider here only data obtained in layer 1 (L1) of the proportional counter units (PCUs), since layer 1 provides the highest signal-to-noise for a relatively soft ($E < 10$ keV) source like $\eta$ Car. Data extraction and instrumental background correction are as described in Ishibashi et al. (1999), Corcoran et al. (2001), and Corcoran (2005), utilizing corrected PCU faint background models[2] to calculate the net rates. All the data presented here were uniformly reduced using the *RXTE* reduction software distributed with the *HEASoft*[3] software package version 6.7, along with calibration data distributed in version 20090817 of the *RXTE* calibration database[4]. Briefly, for each observation, count rates in 16 second bins were extracted from layer 1 for right and left anode chains for each PCU. Instrumental background event files for each

[1]The updated brightness curve is available at
http://eud.gsfc.nasa.gov/Michael.Corcoran/eta_car/etacar_rxte_lightcurve/index.html

[2]see the 2009-12-12 entry in http://heasarc.gsfc.nasa.gov/docs/xte/pca_news.html

[3]see http://heasarc.gsfc.nasa.gov/docs/software/lheasoft/

[4]see http://heasarc.gsfc.nasa.gov/docs/heasarc/caldb/

observation were constructed using appropriate instrumental model backgrounds, and instrumental background lightcurves were extracted from the model background event files again using 16 second time bins. We calculated net count rates for each data bin by subtracting the binned background data from the binned observed gross data. Since casual inspection of the 16-second lightcurves showed no significant variations within any observation, to increase signal-to-noise we calculated average net rates and errors, along with gross source and instrumental background spectra for each observation. These provide the average PCU count rate and spectra of $\eta$ Car (and sources nearby which fall within the $\sim 1^\circ$ FWHM field of view) for each observation. We then converted the net PCU rates to fluxes using the relations given in Corcoran (2005). Figure 1 shows the layer 1 data from all 5 PCUs.

There is additional noise in the apparent X-ray rate in PCU0 and PCU1 subsequent to the loss of the PCU0 propane layer on 2000 May 12 and the loss of the PCU1 propane layer on 2006 December 25; this causes large scatter in the gross PCU0 and PCU1 layer 1 rates, making observations with these PCUs after the propane layer loss difficult to interpret. Additionally PCUs 0, 1, 3, & 4 were switched off for many of the observations. Therefore, in the following analysis we only consider observations from PCU2 Layer 1 since this provides the most uniform and complete set of data.

There are 1224 PCU2 L1 observations analyzed here. The maximum time separation between consecutive observations is 19.5 days, while the minimum separation is only 1 hour. The average exposure time for these 1224 observations is 925 seconds. The minimum exposure was 16 seconds, while the maximum exposure was 2672 seconds. Thirty percent of the observations had an exposure time greater than 1 ksec, and the cumulative exposure time in the PCU2 observations is 1.13 Msec.

## 3. Comparison of Three X-ray Cycles

The *RXTE* PCU2 layer 1 lightcurve of $\eta$ Car is shown in Figure 2. Figure 3 compares the three X-ray minima versus X-ray phase. Phases are calculated using

$$JD(\text{X-ray minimum}) = 2,448,775.792 + 2024E$$

where as usual $E$ is the cycle count. This is the ephemeris from Corcoran (2005) offset by one cycle (2024 days) for convenience. The latest minimum as determined from the PCU2 count rate began on 2009 January 16 (JD 2454847.5, $\phi = 3.0$). The ingress to all three minima are consistent with a period of $2024 \pm 2$ days as given in Corcoran (2005). However, the duration of the 2009 minimum was about one month shorter than the two earlier minima. The recovery from the 2009 minimum began sometime between 2009 February 12

(JD 2,454,874.5, $\phi = 3.013$) and 2009 February 18 (JD 2,454,880.5, $\phi = 3.016$). The exact timing of the recovery is a bit uncertain since the cadence of the observations changed on 2009 February 12 from about once every two days to ∼once per week due to satellite scheduling constraints.

## 4. Color Variations

We calculated hardness ratios for each PCU2 observation. To do this, we first constructed individual detector responses using the `pcarsp` tool distributed with the *HEASoft* software package version 6.7 (which includes a new energy to channel conversion and an improved algorithm for calculating the PCA response) in order to account for gain changes in PCU2 over time. We also used the *RXTE* calibration database (`CALDB`) version 20090817. Use of the improved PCA response algorithms in *HEASoft* 6.7 along with the improved calibration files yields better consistency in spectral parameters across the mission. We then adopted a standard channel-to-energy gain scale, and interpolated each observed PCU2 spectrum as a function of energy onto this scale. In order to provide a background correction, we interpolated the instrumental background spectra for each observation onto the adopted gain scale, and derived net interpolated spectra by subtracting the interpolated instrumental background spectrum from the interpolated observed PCU2 spectrum for each observation. We then calculated hardness ratios ($HR$) from these gain-corrected background-subtracted interpolated spectra as

$$HR = \frac{R(7) - R(3)}{R(7) + R(3)}$$

where $R(7)$ is the net rate at 7 keV (corresponding to channel 15 in the adopted gain scale) and $R(3)$ is the net rate at 3 keV (corresponding to channel 6). Figure 4 compares the variation in $HR$ with the variation in PCU2 net count rate, while Figure 5 compares the hardness ratio between the current cycle (black) along with the previous cycle (green). As seen in Figure 5, the hardness ratios between cycles 1 & 2 are fairly consistent in the phase intervals of overlap for the interval prior to the minima ($1.5 < \phi < 2.0$); however, Figure 5 also shows that, starting at a phase of $\phi \sim 2.2$, the X-ray hardness ratio decreased (i.e. the emission became softer) compared to the previous cycle.

Figure 6 compares the X-ray hardness ratio for each of the three minima. The minimum hardness, $HR = -0.61$, observed by the *RXTE* PCA occurred on 2009 Jan 17 (JD 2454848.71), very near the start of the X-ray flux minimum; this corresponds to the observed time when the contribution of the colliding wind X-ray emission to the PCA spectrum is smallest. There is good consistency in the phasing of the minimum hardness in all three cycles. In each of the cycles there's a notable change which occurs about midway through

the minimum. This variation is most extreme during cycle 3 marking the start of the early recovery. Interestingly the hardness ratios near $\phi = 0.03$ show surprisingly large variations in all 3 cycles, such as the "secondary dip" accompanying the 2003.5 minimum near this phase. In each of the three minima the X-ray hardness increases as the brightness recovers from the minimum state.

The maximum hardness for cycle 3, $HR = +0.03$, was observed on 2009 March 09 (JD 2454900.2, $\phi = 3.026$), 50 days after the minimum hardness. The maximum hardness in cycle 2 was $HR = +0.15$ occurring 83 days after minimum hardness, while in cycle 1 the hardness ratio spiked to its maximum value of $HR = +0.10$ only 57 days after the time of minimum hardness, declined, then increased again. Thus the increase in hardness ratio after the X-ray minimum in cycle 3 occurred earlier than in either cycle 2 or cycle 1 (though only a few days earlier than the cycle 1 $HR$ spike), and the maximum hardness achieved in cycle 3 was less than in either of the two previous cycles. It's worth noting that the maximum hardness ratio observed in cycle 3, the hardness ratio spike in cycle 1, and the "secondary dip" seen in cycle 2 all occur at nearly the same phase, suggesting some type of transition at this phase in the shocked emission soon after periastron passage in each of the three cycles observed. In cycle 3 the hardness ratio declined to $HR = -0.2$ about 52 days after the post-minimum hardness ratio maximum. In cycle 1 and 2, $HR = -0.2$ was not reached until about 70-100 days after the maximum.

## 5. Comparison of the X-ray Spectra at Key Phases

Because of the limited spatial and spectral resolution of the PCA, we used imaging X-ray spectrometry from *CHANDRA*, *XMM*, and *Suzaku* to help constrain the physical change seen in the $\eta$ Car emission at two key phases, one during the recovery and one near apastron. These spectra were obtained as part of a larger set of observations which will be discussed in more detail elsewhere (Hamaguchi et al., 2010, in preparation).

### 5.1. The X-ray Spectrum During the Recovery

In order to better understand the abrupt change in duration of the X-ray minimum, we compared *CHANDRA* (Weisskopf et al. 1996) spectra obtained at nearly the same phase towards the end of the cycle 2 and 3 minima. Figure 7 compares a zeroth-order *CHANDRA* spectrum (in red) obtained on 2009 March 16–17 ($\phi \sim 3.03$) using the high-energy transmission grating spectrometer (HETGS) to a *CHANDRA* spectrum (black) from 2003 August

28 ($\phi \sim 2.03$, one cycle earlier) obtained with the ACIS-S detector (without gratings). As can be seen from Figure 3, the 2009 March 16–17 observation occurred when the source flux had already fully recovered from the X-ray minimum level, while during the 2003 August 28 observation the *RXTE* brightness was still at the "minimum" level. Figure 7 shows the "unfolded" (i.e. corrected for differences in detector response) 2003 March and 2009 August spectra together with the applied model. Note that, below about 3 keV both spectra are significantly contaminated by a "Central Constant Emission" (CCE) component (described more fully in Hamaguchi et al. 2007).

We attempted to model the spectra using a 2-temperature plasma emission model[5] including a Gaussian line at 6.4 keV. For each of the two emission components we also included cold absorption (Wilms et al. 2000) to represent the combined overlying opacity of the stellar winds, the circumstellar nebulosity, and the intervening interstellar medium. While this is a gross oversimplification of the true emission measure distribution as a function of temperature, a two-temperature model is the simplest model which can adequately describe the spectra. Details of the analysis will be presented in Hamaguchi et al. (2010, in preparation).

In order to fit the two spectra, the only difference necessary was that the emission measure of the model that fit the 2003 August 28 ($\phi \sim 2.03$) spectrum needed to be increased by a factor of 12.3 in order to match the 2009 March 16–17 ($\phi \sim 3.03$) spectrum. All other parameters (temperatures and column densities) were the same between the two spectra. This analysis indicates that, at this phase at least, the shape of the spectrum changed little between the 2009 observation and the observation one cycle earlier. The only apparent difference between the 2009 August 28 spectrum and the 2003 March 16–17 *CHANDRA* spectrum (obtained at the same phase in the previous cycle) appears to be an increase in the observed emission measure.

### 5.2. Comparison of Spectra near Apastron from 2000 and 2005

To confirm that the spectral "softening" seen in the *RXTE* colors prior to the 2009 minimum is due to $\eta$ Car and not some other source in the *RXTE* PCA field-of-view, we compared X-ray imaging spectra obtained near apastron in two different cycles. One observation was obtained by *XMM* (Jansen et al. 2001) using the MOS2 instrument on 2000 July 26–28 at $\phi$ =1.47 (obsID: 0112580601, 0112580701; Hamaguchi et al. 2007), while a later observation was obtained on 2006 Feb 3 at $\phi$ =2.47 by *Suzaku* (Mitsuda et al. 2007) using the X-ray XIS0–3 CCD detectors (obsID: 100045010; Hamaguchi et al. 2010, in prep.) Again,

[5]APEC, see http://cxc.harvard.edu/atomdb/

these data are almost exactly one cycle apart. The phasing of these observations are shown in Figure 2. As can be seen in this figure, for most of the phase interval $2.5 < \phi < 3.0$ the star was brighter in X-rays than it was in the previous cycle.

Figure 8 shows the "unfolded" 2000 July 26–28 ($\phi = 1.47$) *XMM* spectrum compared to the "unfolded" 2006 Feb 3 ($\phi = 2.47$) *Suzaku* spectrum. We used other spectra from *XMM* and *Suzaku* obtained near the start of the X-ray minimum (when the colliding wind X-ray source is faintest) to correct for contamination of the colliding wind X-ray spectra by nearby constant emission sources like the CCE and the extended, soft X-ray emission which surrounds the Homunculus nebula (Seward et al. 2001), and which is unresolved to either *XMM* or *Suzaku*. Thus the spectra shown in Figure 8 should represent the emission from the wind-wind collision region. As can be clearly seen in this figure, the hard band flux at energies $E > 2.5$ keV was significantly higher (by a factor of 2) in the 2000 July 26–28 ($\phi = 1.47$) *XMM* spectrum (in black) than in 2006 Feb 3 *Suzaku* spectrum ($\phi = 2.47$, red), suggesting a decrease in the emission measure of the hard source from 2000 to 2006 by a similar factor. The difference between the spectra was smaller in the $E < 2.5$ keV band, but the 2006 spectrum is clearly brighter at these softer energies.

## 6. Discussion

The duration of the 1997–1998 minimum was 81.2 days, while the duration of the 2003.5 minimum was 89.0 days, using the full-width at half maximum (FWHM) statistic as defined in Corcoran (2005). In contrast the FWHM duration of the 2009 minimum was only 53.9 days. While there might be understandable concern that the observed variability is due to contamination from a serendipitous source in the PCU field of view, imaging X-ray spectra obtained by us using the *CHANDRA* X-ray Observatory and from the X-ray Telescope onboard the *Swift* observatory (Pian et al. 2009) confirm that the variable source is indeed $\eta$ Car. As the analysis in section 5.1 shows, the only apparent difference between the 2009 and 2003.5 *CHANDRA* spectra 60 days past the start of the X-ray minimum appears to be an increase in the observed emission measure by about a factor of 12.

As the comparison between the *Suzaku* XIS and *XMM* MOS spectra discussed in Section 5.2 shows, the observed decrease in the hard-band ($E > 5$ keV) flux in the 2006 *Suzaku* spectrum with little change in the softer ($2 < E < 4$ keV) band suggests that the decrease in hardness ratio and flux seen by *RXTE* prior to the cycle 3 minimum ($2.02 < \phi < 2.90$) is produced by a decrease in the emission measure of the hard source (which reduces the emission at $E > 5$ keV) perhaps coupled with decrease in absorbing column (since the emission at $E < 3$ keV did not change very much). Although there's an apparent increase

in the PCU2 hardness ratio during the recovery, this is also mostly due to an increase in the 2–10 keV emission measure rather than a real change in the spectral shape, since, at low flux levels near the X-ray minimum, the soft cosmic background in the PCA dominates over the hard colliding wind emission, so that when the colliding wind source is faint, the *RXTE* spectrum appears softer, and vice-versa. But at phases outside the minimum the observed emission is dominated by the colliding wind source, so the fact that 100 days ($\Delta\phi \sim +0.05$) after the 2009 minimum the PCU2 spectrum was softer than it was 100 days after the 2003.5 minimum is significant.

There are other cycle-to-cycle differences as well (as already noted in Corcoran 2005). Comparison of Figures 2 and 3 shows that, in the interval 620 to 80 days prior to the 2009 minimum, the X-ray flux level was nearly identical to that in a similar interval prior to the 1998 minimum. However, in the 80 days leading up to the 2009 X-ray minimum, the X-ray flux brightened and was nearly identical to the flux level in the 80 days prior to the 2003.5 minimum. Thus, the flux level seen in the 2009 cycle was intermediate between the preceding two cycles. The maximum X-ray flux that has yet been observed by any X-ray observatory occurred just prior to the 2009 minimum on 2008 December 06 (JD 2,454,806.625) when the 2–10 keV flux reached $f_x = 2.8 \times 10^{-10}$ ergs s$^{-1}$ cm$^{-2}$, which corresponds to a luminosity of $\approx 1.8 \times 10^{35}$ ergs s$^{-1}$, assuming a distance of 2300 pc.

As seen in Figure 4, prior to each minimum, the X-ray color mimics the X-ray flux variation – i.e the hardness increases along with the X-ray flux as the time of ingress to the minimum approaches, and then the hardness ratio declines along with the X-ray flux to the start of the minimum. As noted above, this decline in hardness is dominated by the increasing relative contribution of the soft cosmic X-ray background to the observed $\eta$ Car spectrum in the PCU2 field of view as the hard flux from the colliding wind source declines. A noticeable difference between the behavior of the X-ray flux and X-ray hardness is that the value of the X-ray hardness ratio prior to the minimum is similar to the value of the hardness ratio after the minimum, while the X-ray flux prior to the minimum is about a factor of three larger than the value after the minimum. There is also a significant difference in the observed variability of the X-ray hardness during the minimum compared to the X-ray flux. During the minimum, the X-ray flux is fairly constant at a level of about $5.7 \times 10^{-12}$ ergs cm$^{-2}$ s$^{-1}$ (which mostly represents the level of cosmic X-ray background contamination in the PCU2 field of view). On the other hand, midway through the X-ray minimum, the X-ray hardness increases in each of the 3 cycles. In cycle 3 this mid-minimum X-ray hardness increase continues through the early recovery. The timing of this change in X-ray color approximately corresponds to the change from the "deep minimum" to the "shallow minimum" as described by Hamaguchi et al. (2007). This transition probably means that either the shock has intrinsically changed state, or our line of sight to the shocked region

undergoes an abrupt change at this phase.

To understand the change in the duration of the X-ray minimum, and other cycle-to-cycle differences, we need to understand the mechanism(s) responsible for the X-ray minimum – see Hamaguchi et al. (2007) for a discussion of plausible mechanisms. Simple eclipse models (in which the X-ray minimum is produced by the eclipse of the X-ray emitting region by the wind or photosphere of $\eta$ Car) have trouble reproducing the breadth of the eclipse (Ishibashi et al. 1999; Parkin et al. 2009), unless the emitting region near periastron passage is small and located near the stagnation point of the colliding wind flow (Okazaki et al. 2008). If this is not the case, then changes in the wind collision near periastron due to an increase in mass loss rate (Corcoran et al. 2001), inhibition of the companion's wind by gravitational accretion (Soker 2005; Akashi et al. 2006; Kashi & Soker 2009) or radiative inhibition or radiative braking of the companion's wind (Parkin et al. 2009) may be needed. All these models depend on accurate knowledge of the stellar, wind and orbital parameters.

Making the reasonable assumption that the orbital parameters have not changed over the last 15 years, the changes in the X-ray emission recorded by *RXTE* suggest a significant change in either the wind of $\eta$ Car or its companion star due to some change in the underlying stellar parameters (like luminosity, surface temperature, or some combination). The variation observed in the *RXTE* lightcurve and hardness ratio curve, especially the early recovery from X-ray minimum, may suggest a significant change in the system mass loss; the "softening" of the spectrum seen in cycle 3 suggest that this change happened some time after the cycle 2 periastron passage. Whether the changes we see are due to changes in $\eta$ Car or the companion star remain to be determined. Comparison of the *Suzaku* and *XMM* spectra near apastron in cycles 2 and 3 suggest that the softening of the X-ray spectrum is produced by a decrease in the hard-band flux from the shocked companion's wind, possibly coupled by a drop in the absorbing column density at low energies. Comparison of the two *CHANDRA* spectra obtained 60 days after the X-ray minima of cycle 2 and cycle 3 shows that the spectral shape has changed little between the two cycles, but that the flux from the shocked companion's wind increased by an order of magnitude during the cycle 3 recovery .

The cycle-to-cycle change in flux and hardness ratio may be an indication of a change in the emission measure of the hot shocked companion wind, which could in principal be produced by a change in the mass loss rate from $\eta$ Car or its companion. Given its history of instabilities, $\eta$ Car seems to be the more likely suspect. The emission measure $EM$ of the companion's wind scales like $EM \sim 1/r$, where $r$ is the distance from the companion to the stagnation point of the colliding wind flow. The distance of the companion to the stagnation point is

$$r = \sqrt{\eta}/(1 + \sqrt{\eta})D$$

(Usov 1992) where $\eta = \dot{M}_c v_c/(\dot{M} v)$ and $r$ is measured from the primary star, and the subscript $c$ denotes the values for the companion star. We consider the changes in the near-apastron X-ray spectrum as measured by *XMM* and *Suzaku*, and define $R = r_{2006}/r_{2000}$ as the ratio between the distance from the companion to the stagnation point measured by *Suzaku* in 2006 Feb 3 ($\phi$ =2.47) compared to the *XMM* 2000 July 26–28 ($\phi$ =1.47) spectrum. Since the emission measure varies like $1/r$, then $R = EM_{2000}/EM_{2006} \approx 2$ from the comparison of the emission measures of the *XMM* and *Suzaku* spectra discussed in Section 5.2. Let $x = 1/\sqrt{\eta}$ and $x_{2000} = B x_{2006}$, then

$$x_{2006} = \frac{1-R}{R-B} = \frac{1}{B-2}$$

since we observe R=2. Since $x_{2000}/x_{2006} > 0$, then $B > 2$ and $B^2 = x_{2000}^2/x_{2006}^2 = \eta_{2006}/\eta_{2000} = \dot{M}_{2000}/\dot{M}_{2006}$, if the only thing that changed from 2000 to 2006 is $\dot{M}$. Thus $\dot{M}_{2000} > B^2 \dot{M}_{2006}$ or that $\dot{M}_{2000} \gtrsim 4\dot{M}_{2006}$. A factor of 4 decrease in $\dot{M}$ from 2000 to 2006 is surprisingly large. Martin et al. (2010) suggested a mid-cycle decrease in $\eta$ Car's mass loss rate and wind terminal velocity based on changes in visible-band and UV photometry and spectroscopy, though they estimated only a 20% decline in $\dot{M}$ and wind velocity. However, more recently Mehner et al. (2010) showed marked weakening of Fe II, [Fe II], Cr II, and [Cr II] emission lines occurring sometime in 2009, which might be evidence of a far larger decrease in $\eta$ Car's mass loss rate. Kashi & Soker (2009) also required a factor of $\sim$ 2 decrease in mass loss rate in 2009 to explain the early exit from the X-ray minimum using their accretion model.

The wind of $\eta$ Car is believed to be latitudinally-dependent (Smith et al. 2003), and if so it may not be too surprising that the variation in $\eta$ Car's wind properties might be more extreme in the X-ray band than in other bands, if the X-rays probe the local wind state over a limited range of stellar latitudes where the wind variability may be larger. In principle, a decrease in the photospheric luminosity of $\eta$ Car could produced a significant change in mass loss rate, though recent photometry suggests that $\eta$ Car itself is becoming brighter, not fainter (Davidson et al. 1999; Fernández-Lajús et al. 2009).

Finally, an alternative interpretation is that the narrower duration of the 2009 minimum is the "normal" state, and that the previous two minima were of unusually long duration. This interpretation is suggested since many colliding wind models of the X-ray lightcurve produced minima that are much narrower than the minimum observed in 1997. For example, Figure 9 shows a comparison of the model by Parkin et al. (2009) using a 3-D dynamic model of the $\eta$ Car colliding wind shock, attenuated by the intervening absorption from the wind of $\eta$ Car. The model X-ray minimum is much narrower than the minima in 1998 and 2003.5, but closer to that of the 2009 minimum (though even here the observed minimum is a bit

broader than the model). This may be a clue that in 2009 the dominant cause of the X-ray minimum was intervening absorption by the wind of $\eta$ Car, and that the minima in 1998 and 2003.5 were of unusually long duration due to an additional mechanism which suppressed the X-ray emission for an extended period. The delayed X-ray rise in the earlier minima could have been caused by radiative inhibition and/or the collapse of the colliding wind shock (as already suggested by Parkin et al. 2009), though it's not clear at the moment why radiative inhibition of the companion's wind, or the collapse of the bow shock, would have been less effective in 2009 than in 2003.5 or 1998.

## 7. Conclusion

We present our continued monitoring of the 2–10 keV X-ray emission of $\eta$ Car, a supermassive colliding wind binary system, from observations obtained by PCU2 on *RXTE* through its most recent X-ray minimum in January 2009. These data show that the recovery from the 2009 X-ray minimum was surprisingly abrupt, so that the minimum was about 1 month shorter than the 1998 and 2003.5 minima. The *RXTE* monitoring also reveals that the X-ray hardness seems to have declined in the 2004-2009 interval, i.e. in mid-cycle sometime after periastron passage when $\eta$ Car and its companion star are well separated. We suggest that these changes are produced by a decline in mass loss rate of $\eta$ Car's wind, though the rather large changes observed from cycle-to-cycle in the X-ray spectra require a rather large change in $\eta$ Car's wind momentum flux $\dot{M}V_\infty$ of about a factor of four. A drop in mass loss rate may be due to a change in $\eta$ Car's latitudinally-dependent wind, possibly driven by a significant decline in $\eta$ Car's intrinsic luminosity. However at this point we cannot fully rule out changes in the companion star as the cause of the cycle-to-cycle differences seen in the X-ray band. We note that the large-scale change in $\eta$ Car's mass loss rate, unprecedented since the end of the 19th century, needs to be confirmed by additional observations at X-ray and lower energies.

## REFERENCES

Akashi, M., Soker, N., & Behar, E. 2006, ApJ, 644, 451

Bradt, H. V., Rothschild, R. E., & Swank, J. H. 1993, A&AS, 97, 355

Corcoran, M. F. 2005, AJ, 129, 2018

Corcoran, M. F., Ishibashi, K., Swank, J. H., & Petre, R. 2001, ApJ, 547, 1034

Damineli, A., Hillier, D. J., Corcoran, M. F., Stahl, O., Levenhagen, R. S., Leister, N. V., Groh, J. H., Teodoro, M., Colombo, J. F. A., Gonzalez, F., Arias, J., Levato, H., Grosso, M., Morrell, N., Gamen, R., Wallerstein, G., & Niemela, V. 2008, MNRAS, 384, 1649

Davidson, K., Gull, T. R., Humphreys, R. M., Ishibashi, K., Whitelock, P., Berdnikov, L., McGregor, P. J., Metcalfe, T. S., Polomski, E., & Hamuy, M. 1999, AJ, 118, 1777

Davidson, K., & Humphreys, R. M. 1997, ARA&A, 35, 1

Fernández-Lajús, E., Fariña, C., Torres, A. F., Schwartz, M. A., Salerno, N., Calderón, J. P., von Essen, C., Calcaferro, L. M., Giudici, F., Llinares, C., & Niemela, V. 2009, A&A, 493, 1093

Hamaguchi, K., Corcoran, M. F., Gull, T., Ishibashi, K., Pittard, J. M., Hillier, D. J., Damineli, A., Davidson, K., Nielsen, K. E., & Kober, G. V. 2007, ApJ, 663, 522

Hillier, D. J., Davidson, K., Ishibashi, K., & Gull, T. 2001, ApJ, 553, 837

Ishibashi, K., Corcoran, M. F., Davidson, K., Swank, J. H., Petre, R., Drake, S. A., Damineli, A., & White, S. 1999, ApJ, 524, 983

Jansen, F., Lumb, D., Altieri, B., Clavel, J., Ehle, M., Erd, C., Gabriel, C., Guainazzi, M., Gondoin, P., Much, R., Munoz, R., Santos, M., Schartel, N., Texier, D., & Vacanti, G. 2001, A&A, 365, L1

Kashi, A., & Soker, N. 2009, ApJ, 701, L59

Langer, N. 1998, A&A, 329, 551

Martin, J. C., Davidson, K., Humphreys, R. M., & Mehner, A. 2010, AJ, 139, 2056

Mehner, A., Davidson, K., Humphreys, R. M., Martin, J. C., Ishibashi, K., Ferland, G. J., & Walborn, N. R. 2010, ApJ, 717, L22

Mitsuda, K., et al. 2007, PASJ, 59, 1

Moffat, A. F. J., & Corcoran, M. F. 2009, ApJ, 707, 693

Okazaki, A. T., Owocki, S. P., Russell, C. M. P., & Corcoran, M. F. 2008, MNRAS, 388, L39

Parkin, E. R., Pittard, J. M., Corcoran, M. F., Hamaguchi, K., & Stevens, I. R. 2009, MNRAS, 394, 1758

Pian, E., Campana, S., Chincarini, G., Corcoran, M. F., Hamaguchi, K., Gull, T., Mazzali, P. A., Thoene, C. C., Morris, D., & Gehrels, N. 2009, ArXiv, 0908.2819, 1

Pittard, J. M., & Corcoran, M. F. 2002, A&A, 383, 636

Seward, F. D., Butt, Y. M., Karovska, M., Prestwich, A., Schlegel, E. M., & Corcoran, M. 2001, ApJ, 553, 832

Smith, N. 2008, Nature, 455, 201

Smith, N., Davidson, K., Gull, T. R., Ishibashi, K., & Hillier, D. J. 2003, ApJ, 586, 432

Smith, N., Li, W., Foley, R. J., Wheeler, J. C., Pooley, D., Chornock, R., Filippenko, A. V., Silverman, J. M., Quimby, R., Bloom, J. S., & Hansen, C. 2007, ApJ, 666, 1116

Soker, N. 2005, ApJ, 635, 540

Usov, V. V. 1992, ApJ, 389, 635

Weisskopf, M. C., O'dell, S. L., & van Speybroeck, L. P. 1996, in Presented at the Society of Photo-Optical Instrumentation Engineers (SPIE) Conference, Vol. 2805, Society of Photo-Optical Instrumentation Engineers (SPIE) Conference Series, ed. R. B. Hoover & A. B. Walker, 2–7

Wilms, J., Allen, A., & McCray, R. 2000, ApJ, 542, 914

*Facilities:* CXO, Suzaku, XMM, RXTE

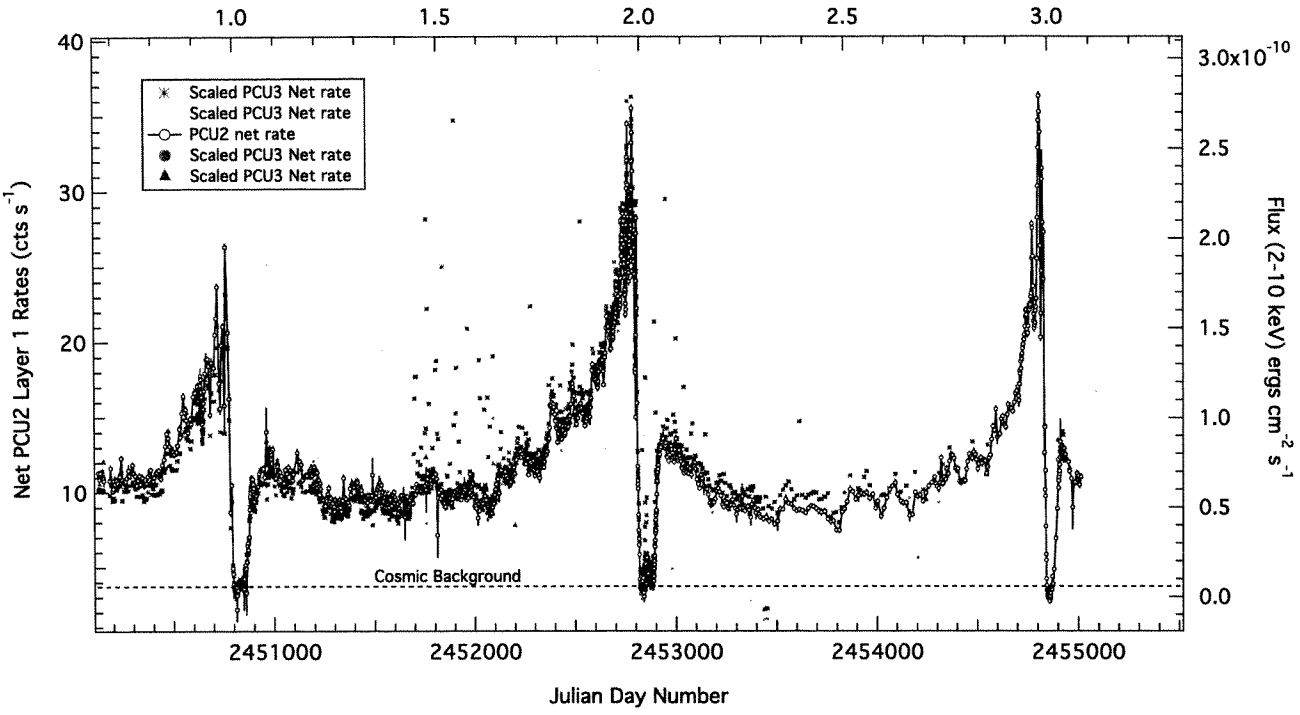


Fig. 1.— The *RXTE* layer 1 X-ray lightcurve, 1996-2009, for all Proportional Counter Units. The PCU2 data are plotted as net rates, while the PCU0, 1, 3 & 4 data are scaled to flux using the conversion relations given in Corcoran (2005). An estimate of the cosmic background is shown by the dotted line, which limits the sensitivity of *RXTE* to measure the true flux level during the X-ray minimum.

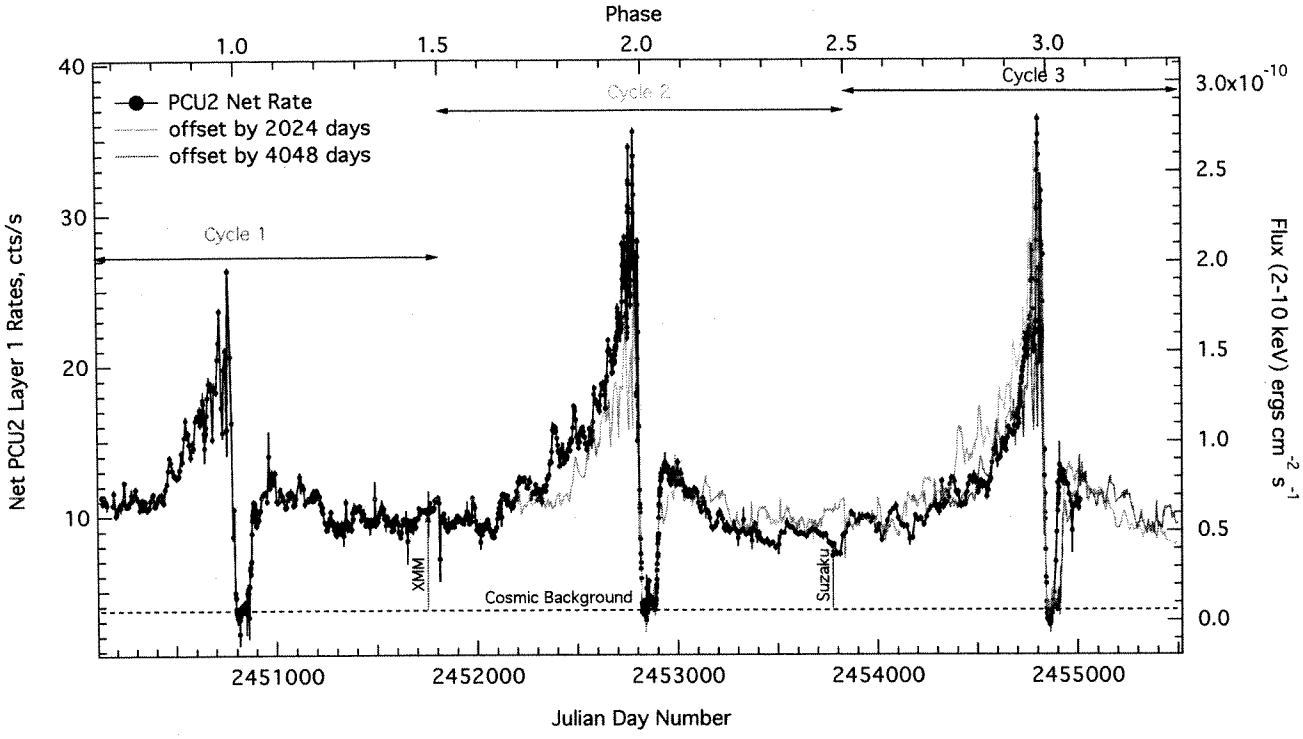


Fig. 2.— The *RXTE* PCU2 layer 1 X-ray lightcurve, 1996-2009. Cycles 1, 2 and 3 are defined (roughly) as apastron to apastron ($N - 0.5 < \phi < N + 0.5$, where $N$ is the cycle number). Cycle 1 includes the 1998 minimum, cycle 2 includes the 2003.5 minimum and cycle 3 the 2009 minimum. The data in green and red have been offset by 2024 and 4048 days, respectively, to facilitate comparison of flux in different cycles. Blue arrows at $\phi = 1.47$ and $\phi = 2.47$ indicate the phasing of the *XMM* and *Suzaku* spectra, respectively, discussed in Sec. 5.2

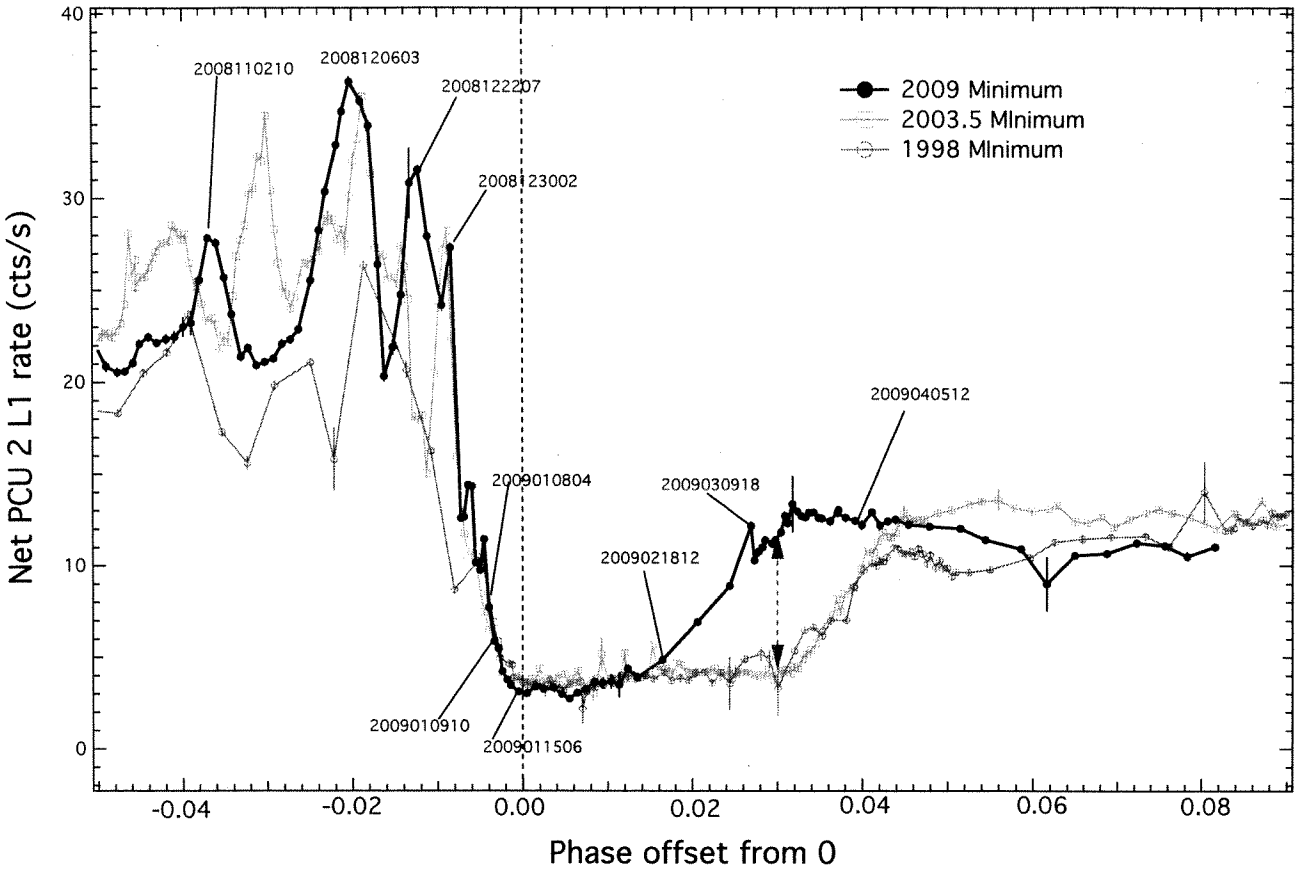


Fig. 3.— Comparison of the three minima observed by *RXTE*. As discussed in the text, the 2009 minimum (black) ended about one month earlier than the previous two minima observed by *RXTE*. Particular *RXTE* observations are marked by the observation date in YYYYMMDDHH format. A blue dashed arrow shows the phasing of the 2009 and 2003 *CHANDRA* spectra discussed in Section 5.1.

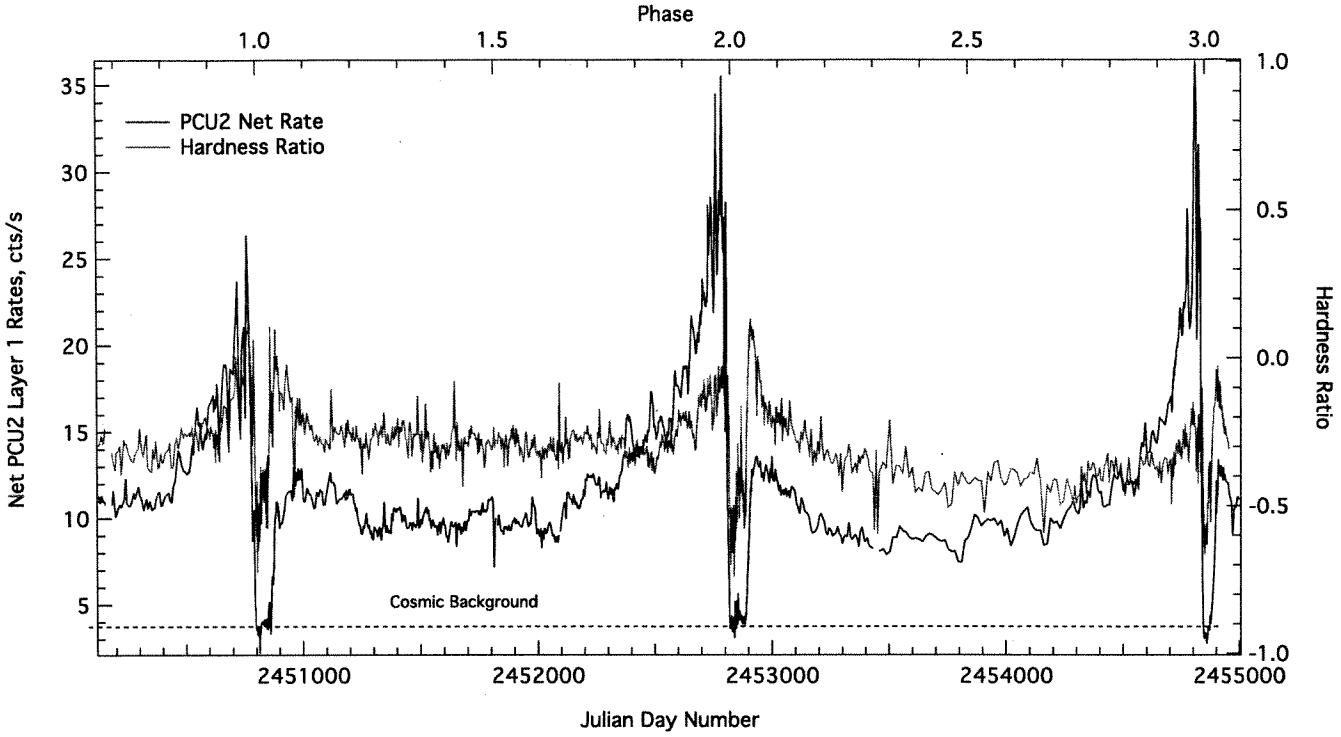


Fig. 4.— Comparison of the variation in spectral hardness measured by PCU2 compared to the flux variation.

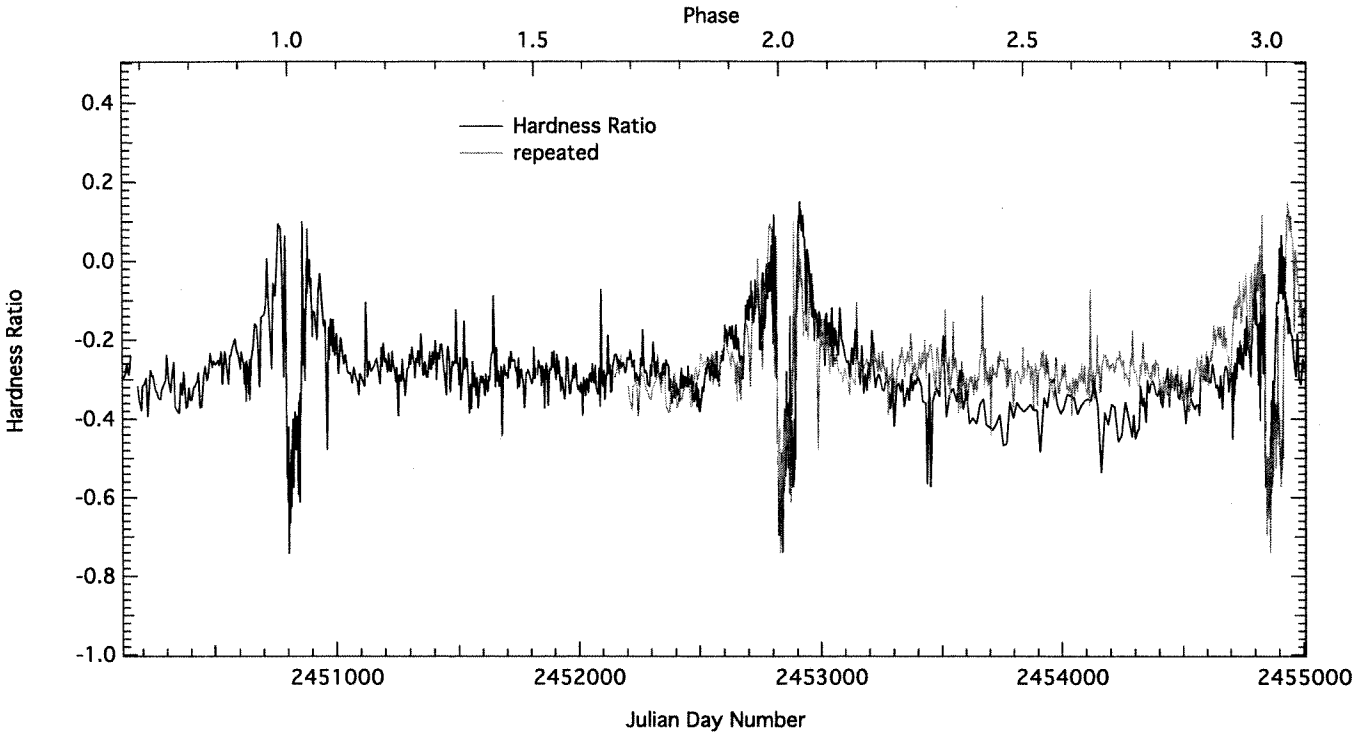


Fig. 5.— Comparison of the PCU2 color from cycle-to-cycle. The green data shows the color variations advanced by 1 cycle.

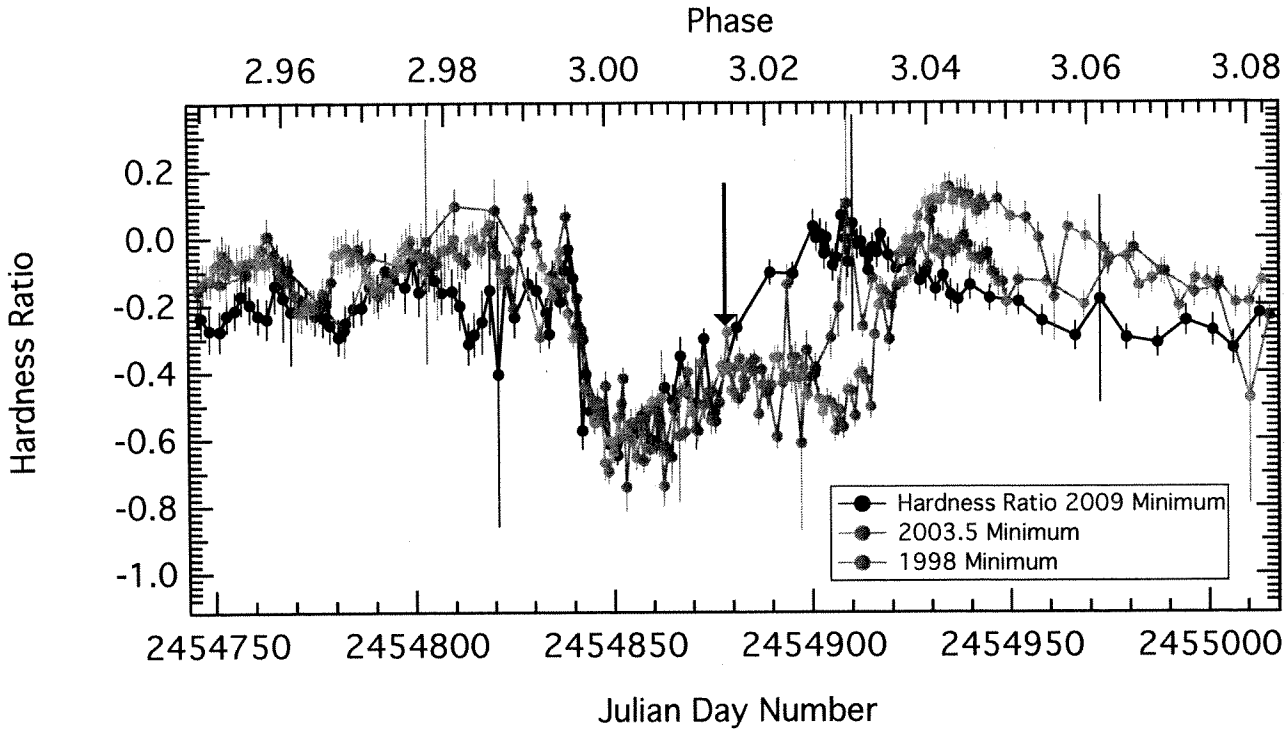


Fig. 6.— Comparison of the variation in spectral hardness measured by PCU2 for the three flux minima observed by *RXTE*. The arrow shows the approximate transition between the "deep minimum" and the "shallow minimum" states (see Hamaguchi et al. 2007). The time scale corresponds to the black data points while the times corresponding to the 1998 and 2003.5 minimum data have been advanced by 4048 and 2024 days, respectively. Some spikes in hardness prior to the X-ray minimum are real and are associated with spikes in the X-ray flux, as discussed in more detail in Moffat & Corcoran (2009).

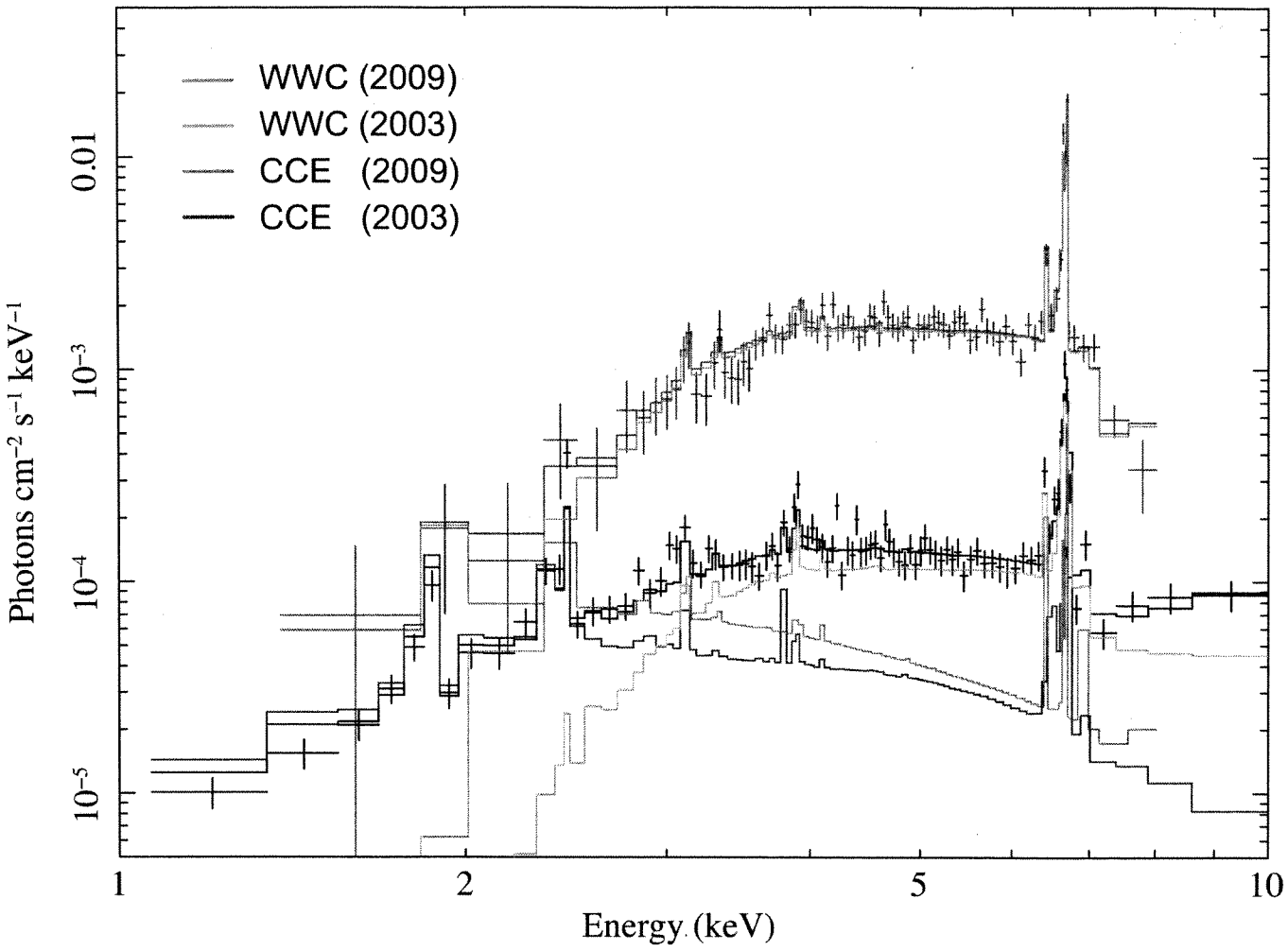


Fig. 7.— Unfolded X-ray spectra during X-ray minima in 2003 (*CHANDRA*/ACIS-S: *black*) and 2009 (*CHANDRA*/HETG: *red*). The solid black and red lines show the best-fit models. These models include a "Wind-Wind Collision" (WWC) component (which includes two thermal plasma emission models with independent absorptions) plus a contaminating source, the "Central Constant Emission" (CCE) component discovered by Hamaguchi et al. (2007) (and which is only important at energies below 3 keV when the source is in the faint state). The fixed CCE components, estimated from spectra during the deep minima, and the best-fit WWC components are shown individually. The 2003 model also includes an approximate correction for photon pileup in the *CHANDRA* CCD spectrometer.

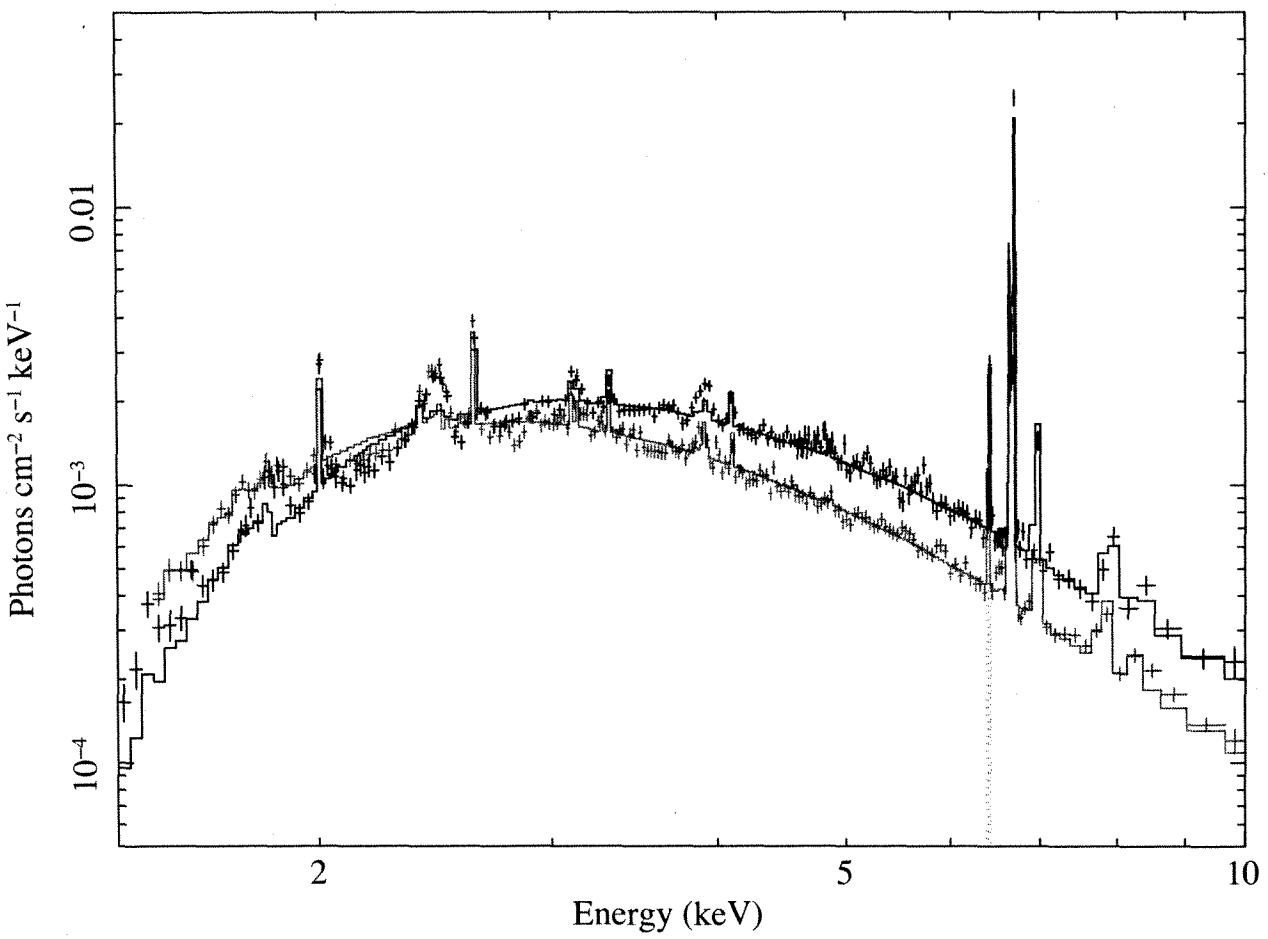


Fig. 8.— Unfolded X-ray spectra during near apastron in 2000 (*XMM*: *black*, $\phi = 1.47$) and 2006 (*Suzaku*: *red*, $\phi = 2.47$) after subtracting background estimated from the deep X-ray minimum observations. The solid lines show the best fits using an absorbed 1-temperature model, which adequately represents the continuum shape but does a poor job describing the ratio of the H-like to He-like lines.

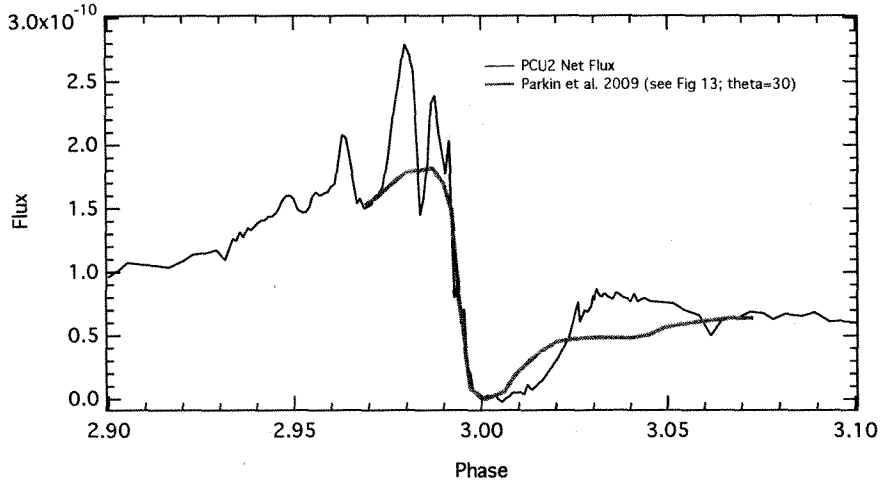


Fig. 9.— Comparison of the *RXTE* 2009 minimum and a model of the attenuated 210 keV X-ray emission by Parkin et al. (2009). The model parameters assume the angle between the projected line of sight and the major axis $\theta = 30°$, an inclination $i = 42°$ $e = 0.9$, and $\eta = 0.18$, where $\eta$ is the ratio of the wind momentum flux of the secondary to the primary (i.e., $\eta = \dot{M}_c V_{\infty,c}/\dot{M}_1 V_{\infty,1}$, where the subscript $c$ refers to the secondary star). Both the *RXTE* data and the model curve have been adjusted to remove an estimate of the cosmic background contamination in the field of view of the *RXTE* PCA.